

# PREPARATION OF PRECIPITATED IRON FISCHER-TROPSCH CATALYSTS

Burtron H Davis<sup>1</sup> and Freddie L. Tungate<sup>2</sup>

<sup>1</sup>Center for Applied Energy Research  
University of Kentucky  
3572 Iron Works Pike  
Lexington, KY 40511

<sup>2</sup>United Catalysts, Inc.  
P. O. Box 32370  
Louisville, KY 40232

DOE Contract #DE-AC22-91PC90056

Starting Date: December 18, 1990

Ending Date: December 17, 1993

## OBJECTIVE

The objective of this project is to investigate the role of preparation, washing, drying and/or calcination, mode of promoter addition, and method of activation upon the initial activity, selectivity and resistance to aging of precipitated iron catalysts used in the Fischer-Tropsch synthesis. The various parameters given above are to be optimized to develop a process design for the continuous preparation of precipitated iron catalysts that ensures uniformity in catalytic properties from one batch of catalysts to the next. The deliverable at the end of the contract is a process flow sheet, plant design and cost estimate for construction of a plant that will produce 100 pounds of catalyst per week.

## INTRODUCTION

Much of the early work on the FTS was carried out in Germany. Among the reasons for this were the discovery by German researchers, the earlier success in Germany with the development of a high pressure process for ammonia synthesis from nitrogen and hydrogen, and the lack of significant petroleum reserves in Germany. The first catalysts tested by Fischer were prepared by mixing the metal oxides of the dissolved or melted metal nitrates. The latter procedure appeared to be somewhat more efficient. The oxides were then reduced with pure hydrogen at about 350° C. At first, the oxides were used in the form of fine powders, which were difficult to handle. For this reason, the oxide mixture was sometimes pressed into a cake and broken into granules, sometimes compressed under pressure with a binder such as starch, and sometimes deposited on a carrier such as ceramic pieces, asbestos, clay chips, pumice stone, or activated charcoal. It was thought that the carrier might also help to preserve the surface of the catalyst. However, this was not so, for iron deposited on asbestos, for example [1].

An area of investigation that had a major impact upon the preparation of iron based catalysts was the fundamental and process development studies that led to the smooth-working commercial ammonia synthesis process. While the initial discovery was made with an osmium catalyst [3], it was realized that a less expensive catalyst had to be developed if the original discovery could be utilized to provide a feasible commercial process. After years of work, investigations headed by Mittasch led to the introduction of an iron based catalyst [4]. It was the development of this catalyst that enabled the Germans to develop a commercial process for ammonia synthesis.

In the United States, the advent of WWI caused legislative leaders to recognize the vulnerability of our Nation to the import of nitrates from Chile. As a long-term solution to this problem, Congressional leaders were successful in providing funds for a serious research and development effort in synthetic ammonia synthesis [5]. First, a significant effort was undertaken to develop a catalyst that would have sufficient activity and stability to match that of the catalysts used by the German processes. In order to accomplish this goal the Fixed Nitrogen Laboratory was organized and given the task of developing such a catalyst. The laboratory attained the goal set for it in an astonishing short time. In part, this was due to the willingness of the Congressional leadership to continue to provide the needed funding even though the end of WWI in 1918 removed the immediate threat to the import of nitrates from Chile, and thereby the immediate need for a U.S. to develop a synthetic ammonia industry. Another reason for the rapid success was the superb leadership of the R & D effort which included F. G. Cottrell, who later developed the precipitator named after him. By 1925, just six years following the start-up of the laboratory, the group at the Fixed Nitrogen Research Laboratory had shown that doubly promoted iron catalysts containing about 3% aluminum oxide and one percent potassium oxide were entirely satisfactory for commercial use and would, if operated on pure gas, have a very long life. Actually, many similar commercial catalysts are said to retain their activity for more than 5 years [6]. Not only was an active catalyst developed and evaluated but an "American Process for Ammonia Synthesis" was designed and described [7]; furthermore, the government subsidized the construction of a commercial plant [5]. This was a massive effort that in today's dollars approach the magnitude of the resources needed for a full scale direct or indirect coal liquefaction plant. The development of the ammonia process may be cited as a model of "how a government should develop technology and processes".

Paul H. Emmett recalled a story, possibly a slight embellishment of the actual case, but one that still illustrates the uncertainties associated with catalyst preparation, about the early years of the U.S. effort. It was known to the American workers that the Germans added nonreducible oxide to their iron catalyst. However, after much testing with iron catalysts containing various amounts of a variety of irreducible oxides, a suitable catalyst could not be made. It was only after the Americans started adding a second component, and especially an alkali or alkali-earth metal oxide, that a suitable catalyst could be prepared. The reason for this, according to Emmett, was that the Americans utilized water purified by distillation for their catalyst preparations. The Germans, on the other hand, utilized "tap" water which, in this instance, contained sufficient alkali to provide the needed second promoter. In any event, Larson and coworkers obtained several patents

covering doubly promoted and related catalysts during the period 1925-1934. Many of the catalysts for the ammonia synthesis were prepared by the fused method.

The Germans initiated commercial-scale reactors in 1943 to be able to make comparisons between the cobalt and iron catalysts. The first test at Schwarzheide and all subsequent war-time tests employed precipitated-iron catalysts except for I. G. Farbenindustrie who used, for the first time according to Pichler and Hector [2], a fused ammonia-type catalyst. Although the results appear to have been good, iron catalysts were not used until after WWII.

Interest in the FTS developed in the U.S. during the late 1930s. Hydrocarbon Research, Incorporated (HRI) acquired world-wide rights, excluding Germany, for the Ruhrchemie FTS process. HRI undertook work on this but appear to have only made confirmatory experiments prior to WWII, and little, if any, work was done on this process during WWII. Following WWII, with U.S. fuel consumption at an all-time high, HRI vigorously pursued FTS work. The high versatility of the iron catalysts resulted in the development of various types of iron catalysts which could be used as a fixed-bed catalyst, a fixed fluid-bed catalyst, an entrained fluid-bed catalyst, a slurry-type catalyst, and as an oil-submerged catalyst. HRI's work led to a pilot plant at Brownsville, Texas. The process utilized a fixed, fluidized-bed reactor system. As raw materials for catalyst preparation, iron ore or millscale, obtained from steel-mill rolling operations, was used. These raw materials were processed to contain ca. 0.5-1.0% potassium and structural promoters, if needed. The material was ground to 40-325 mesh and reduced with dry hydrogen prior to use. A number of U.S. companies were involved with the Brownsville plant prior to its closing the plant in the late 1950s.

Some of the most detailed and well-planned research in the U.S. relating catalyst composition and catalyst preparation to catalytic properties was done at the Bureau of Mines laboratory. Anderson summarized much of the work on iron catalysts that was carried out up to about 1955 [8].

Catalyst preparation is one of the least understood aspects of the science of catalysis. This is true whether the objective is to prepare crystalline materials such as zeolites or to prepare amorphous materials. At the heart of the problem is the fact that the preparation of these materials involves a complex polymerization process. One normally begins with a solution that contains a monomer that is comprised of a single metal ion, and manipulates the solubility by the addition of a second component. A widely employed procedure involves the adjustment of the pH of an aqueous solution to effect polymerization. A number of factors may impact the reaction pathway and the properties of the final product; included among these are the valence of the metal ion, the nature of the anion, the pH, temperature and rate of precipitation, the extent of precipitate aging, the extent and manner of washing of the precipitate, the lower temperature to effect removal of most of the water entrapped during preparation and the temperature and conditions for the calcination.

A number of synthetic approaches were utilized to provide materials for testing in Fischer-Tropsch Synthesis (FTS). These included, in addition to precipitated catalysts: (1) the fused-type of catalyst that was developed for ammonia synthesis; (2) sintered materials where an iron oxide paste is compacted, formed and then sintered; (3) cemented materials where a component such as alumina or silica is added to an iron oxide to serve to cement the particles together during calcination; and (4) catalysts prepared from a variety of natural ores and manufacturing by-products. Extensive tests were made at the Bureau of Mines Pittsburgh Laboratory on all of the above types of catalytic materials. It appears that, with sufficient effort, any of the above preparative techniques could be utilized to prepare a catalyst that would match the "best" prepared by another method unless a basis for comparison is "life of the catalyst".

The early philosophy of catalyst preparation cannot be summarized better than was done in 1956 by Professor Anderson: "In most precipitated iron catalysts, the iron is present initially as ferric oxide or magnetite gels. Due to the complex colloidal chemistry involved, elaborate methods of preparation were developed. Although in many cases these procedures seem very complicated, they were usually the result of laborious empirical research and represent practical ways of attaining the desired gel structure and obtaining precipitates that can be filtered and washed free of foreign ions without undue effort. However, the cost of preparing precipitated catalysts by any of the procedures is relatively high [9].

A number of factors contribute to the relatively high cost for the precipitated catalyst that is referred to by Professor Anderson. Contributing to the cost of the precipitated catalyst is the large volume of liquid involved in the precipitation, the formation of a precipitate that is difficult to handle under the best of conditions and exasperating under the worst conditions; the large volume of materials and the large number of consecutive operations that were involved in washing the precipitate; the difficulty and slowness of collecting the precipitate; the extrusion or other procedure to produce a certain catalyst form if desired; the amount of water required to be removed from the precipitate in the drying procedure; the need for a slow heating rate at low moisture exposure during the calcination step; and the amount of grinding and sizing to produce the final catalyst form. The fused catalyst, on the other hand, could be prepared with much fewer steps: the oxide was melted at high temperature with an electric current; the promoters were added as a solid cake and was dispersed into the melt; the melt was poured to form chunks that could be ground and sized; undersized material could be readily recycled by addition to the next batch. This latter point, the production of little waste, has become more important and today the need, on a commercial scale, to approach zero waste will make the precipitation technique of catalyst preparation a demanding task.

It has been established time and time again that an iron catalyst, if it is to have sufficient activity, selectivity for alkene formation, and catalyst lifetime must contain two additional ingredients: (1) an alkali promoter which will impact the activity, the selectivity for alkene formation, and the molecular weight of the product and (2) a non-reducible structural additive that is essential for maintaining a useful catalyst lifetime. Thus, the factors to be

controlled in the preparation of the iron catalyst are how does one prepare the metal oxide precipitate as well as how and in what order are the other two components added.

The current understanding of catalyst preparation indicates that a preferred catalyst requires that precipitation be carried out rapidly. In general, rapid precipitation produces disorder in the resulting solid and is expected to produce the smallest particles that can be prepared by a precipitation technique. If the method is to produce materials of high surface area (200-300 m<sup>2</sup>/g), the individual particles will be in the colloidal range. These particles must be agglomerated with a minimum of crystal growth if filtration is to be utilized to collect the precipitate for further processing. Two approaches are possible: precipitate or age briefly at elevated temperatures or use a highly charged coagulant. Both approaches will have to be tested in any study that defines a preferred method for scale-up for catalyst preparation. It is quite likely that the preferred approach will be to effect the precipitation itself at elevated temperatures; thus the coagulation process would occur to a significant extent in the precipitation reactor itself. The addition of a material that has a charge and which will be adsorbed by the iron precipitate may effect coagulation. It is known that silica, added as potassium silicate, is essentially completely adsorbed on the surface of the hydrous iron oxide up to a total concentration of a few percent of the amount of iron present. The most effective way to add the non-reducible oxide - in the precipitation step or in a following step - must be determined.

The initial studies shall be to determine the impact of process variables upon the physical properties of the iron oxide produced by precipitation. The variables investigated shall be the final pH of the precipitation mixture, the concentration of the iron and base, the base used (e.g., hydroxide or carbonate, potassium or sodium), the temperature of the precipitation, the time taken to effect the precipitation, the length of time the precipitate is aged prior to filtration, the filtration rate, the method of washing the hydrated iron oxide gel (washing filter cake versus re-dispersion and washing cycles), the fraction of the reagents contained in the hydrous precipitate, the drying and calcination conditions. In these initial studies surface area and pore volume together with the examination by scanning electron microscopy and transmission electron microscopy to determine the particle and agglomerate shapes will be utilized to define the impact of the above variables upon the finished product. Dry [10] contends that the pore structure of the catalyst is largely determined in the very first stage of the catalyst preparation, i.e., the precipitation of the Fe<sub>2</sub>O<sub>3</sub>. According to Dry, if the precipitation conditions are such that the iron oxide has narrow pores, then the final catalyst will also have this feature.

The SASOL experience indicated that only iron catalysts with a large number of narrow pores are effective for producing high yields of heavy wax. This was taken to imply that the primary products (e.g., olefins) should have a long residence time within the catalyst particles so that they can re-adsorb on the catalyst and further chain growth can occur. These catalysts have areas of above 300 m<sup>2</sup>/g and the majority of the pores have diameters below 5 nm. In contrast, the reduced fused catalysts used in the SASOL fluidized bed reactors for producing gasoline and lighter products have areas of ca. 10 m<sup>2</sup>/g with an average pore size of ca. 30 nm. SASOL personnel have extensive

experience with FTS and do produce at a commercial scale both gasoline and diesel products.

## RESULTS AND DISCUSSION

### CHARACTERIZATION OF COMMERCIAL CATALYST

A sample of a commercial Fischer-Tropsch catalyst was characterized in UCFS laboratory and the results are summarized in the following.

The catalyst is a 1/16" extrudate whose length is somewhat excessive. The rule of thumb for extrudates is that the length is 2 to 4 times the diameter; this catalyst, with a length of about 6 mm and a diameter of 1.5 mm ( $L/D = 4.1$ ) falls at the extreme value for this rule. The density (49.5 lbs/CF) is typical for a silica containing transition metal oxide catalyst.

The loss on ignition (LOI) is high at 15.9%, and the catalyst contains residual carbon dioxide, probably as the carbonate. Chemical analysis shows that the catalyst contains 3.80% CuO, 82.8%  $Fe_2O_3$ , 2.56%  $K_2O$ , and 13.3%  $SiO_2$ .

The surface area is high, 277  $m^2/g$ . This value is obtained for the uncalcined, oxide form. Usually the higher area you start with, the more surface area will be retained on reduction. The median pore diameter is 199 Å and is unimodal except for "skin" pores caused by forming. The mercury penetration pore volume greater than 30 Å is 0.52  $cm^3/g$ , which is a high value.

X-ray diffraction shows evidence of both  $\alpha$ - $Fe_2O_3$  and  $CuFe_2O_4$ . A broad peak attributed to amorphous  $SiO_2$  is also observed. The sample is ferromagnetic, suggesting traces of  $\gamma$ - $Fe_2O_3$ .

Some preparation conditions may be inferred from the above data. It is not readily apparent which metal salts were used to make this catalyst although the nitrate would be indicated rather than the chlorides. If the salt used were sulfate this should be determined by an analysis of the exit gas for  $H_2S$  during reduction.

The order of addition is probably salts to base. This is because of the evidence of  $\alpha$ - $Fe_2O_3$ , which is formed at high pH. The base was most certainly potassium carbonate as evidenced by the residual  $CO_2$  analysis; operation so as to absorb a significant amount of  $CO_2$  from the atmosphere during the catalyst preparation would negate this conclusion.

All one can say about the temperature of preparation is that it was probably high, allowing a high degree of solution saturation. This is found from the XRD, which indicates crystallite sizes near the 30-40 Å lower limit of detection, and smaller. The time of mixing cannot be known from the above data, nor can the degree of mixing and the time of

aging. One might guess that the precipitation was rapid, mixing intense, and aging minimal due also to the small crystallite size.

In terms of isolation of the catalyst, one can only say that if potassium carbonate was used, extensive washing by reslurry would be indicated.

When one operates with a fluid bed or slurry phase catalyst, certain properties are needed. The most important of these are shown in the following table. The size, density, and shape for the different modes are shown. What is given as mechanical strength in fixed bed is now more appropriately termed attrition resistance in fluid bed or slurry phase.

TABLE 1. SPECIFIC PREFERRED PROPERTIES FOR DIFFERENT REACTOR TYPES.

	Fixed Bed	Fluid Bed	Slurry Phase
Mechanical Strength	Crush Strength	Attrition	Attrition
Size	> 1.5 mm	70 - 80 $\mu$	2 - 300 $\mu$
Density	0.5 - 2 g/cc	0.7 -1.1 g/cc	0.5 - 1.5 g/cc
Shape	Various	Spherical	Spherical or Granular

Fortunately, there is a piece of equipment which can isolate the catalyst and, under the appropriate conditions, form an attrition resistant particle having a near optimum size, shape, density, and porosity. It is a spray dryer. A spray dryer is just a vessel through which a heated air stream is blown, into which a slurry is atomized. There are two main categories of spray dryers, distinguished by their method of atomization. One uses a rotary wheel atomizer, the other a two-fluid nozzle. In general, wheel atomizers produce a narrower distribution of particle sizes, which two-fluid nozzles offer great variation in particle size.

There are a number of variables in operation of a spray dryer. These and some of their effects on the finished product are given below in Table 2.

Particle size is most sensitive to the degree of atomization. It is generally possible to go as low as 40  $\mu$  and as high as 90  $\mu$  with a wheel. A nozzle gives broader distributions, and can make up to about 120 average sizes.

Inlet and outlet temperature affects the drying rate and porosity/pore size distribution. Air flow rate determines the residence time in the dryer.

The slurry solids, feed rate, and viscosity are important in porosity/pore size distribution as well as attrition resistance. The slurry percent solids will also impact the particle density.

TABLE 2. VARIABLES AND THEIR EFFECTS UPON THE FINISHED PRODUCT.

VARIABLE	EFFECT OF VARIABLE
WHEEL SPEED (Nozzle Size, Air Pressure)	PARTICLE SIZE
INLET TEMPERATURE/ OUTLET TEMPERATURE	DRYING RATE; POROSITY/PSD
GAS FLOW RATE	RESIDENCE TIME
SLURRY % SOLIDS/SLURRY FEED RATE	PRODUCTIVITY/ATTRITION RESISTANCE
SLURRY VISCOSITY	ATTRITION RESISTANCE/POROSITY/ PSD

For a catalyst, the optimization of the spray drying variables to produce the desired product becomes a statistical design experiment which can be truncated somewhat based on experience in the art.

Two other sections will be added: one on three pretreatment methods and one on the precipitation-drying-calcining surface area.

### CATALYST PRETREATMENT

Pretreatment is an important aspect of developing an active and selective catalytic material for the Fischer-Tropsch synthesis. It has been reported that pretreatment in CO results in a better catalyst than one pretreated in hydrogen (a,B, C); however, there is no clear consensus as to which phase provides the superior activity (11-137). A commercial sample of ultrafine iron oxide (United Technologies, surface area 270 m<sup>2</sup>/g) was used for pretreatment studies. A process scheme employing 300 ml continuously stirred tank reactor (CSTR) was used for the study. A slurry of 2.2g of iron oxide was charged to the CSTR. Pretreatment gas (either CO or H<sub>2</sub>) or syngas (H<sub>2</sub>/CO = 1.03) was introduced to the reactor which was then pressurized to 105 psig (8 atm absolute). The temperature of the reactor was then increased from ambient to 260°C at a rate of 1.5°C/min with a gas flow rate of 2.57 NL/g Fe/hr or 5.57 NL/g Fe/hr for the syngas mixture. A stirring rate of 1200 rpm was used. Flow of the activation was continued for a 24 hour period and then a syngas flow (5.57 NL/g Fe/hr) was introduced to the reactor. The exit gas was analyzed to follow CO conversion during activation and synthesis periods. During the activation process and the syngas reaction period, a small amount of catalyst was withdrawn from the reactor as several designated times for X-ray diffraction and electron microscopy studies.



## ACTIVATION IN CO

Figure 1 shows the XRD patterns of the  $\text{Fe}_2\text{O}_3$  catalyst activated in CO for 2, 10 and 24 hr. The untreated  $\text{Fe}_2\text{O}_3$  is amorphous to XRD. According to the manufacture specification, the  $\text{Fe}_2\text{O}_3$  structure determined by electron diffraction is hematite. After 2 hrs of reaction in CO at 260 °C, the catalyst shows XRD peaks at  $2\theta = 30.1, 35.4, 43.1, 56.9$  and  $62.5^\circ$  that are characteristic of  $\text{Fe}_3\text{O}_4$  magnetite (Fig. 1a). Furthermore, weak doublet peaks can also be observed above  $2\theta = 60^\circ$  (e.g. peaks at ca.  $2\theta = 90^\circ$ ), indicating the presence of  $\text{Fe}_2\text{O}_3$  magnetite. Two additional peaks at  $2\theta = 38.0$  and  $45.0$ , which are not due to the magnetites, were also observed; these can be attributed to the two most intense peaks of  $\text{Fe}_3\text{C}$  cementite ( $2\theta = 37.8$  and  $45.1^\circ$ ). The peak at  $45.0^\circ$  is also coincident with the most intense XRD peak of  $\alpha\text{-Fe}$ . With further conversion in CO, several changes in the XRD pattern of the catalyst can be noted by comparing Figure 1b (10 hr in CO) and 1c (24 h in CO) with 1a:

- (1) The XRD peaks at  $2\theta = 30, 35, 43$  and  $62.5^\circ$  become broad; indicating the formation of new iron phases;
- (2) a new, weak peak at  $31^\circ$  was observed that, together with the observation in (1) above, suggests that maghemite  $\text{Fe}_2\text{O}_3$  is the new phase since maghemite shows XRD peaks near  $31, 35, 43$  and  $62^\circ$ ;
- (3) the peak at  $56.9^\circ$  decreases with reaction time; this peak can be used as an indication of the presence of  $\text{Fe}_3\text{O}_4$  magnetite; therefore, the decrease in intensity of the  $56.9$  peak suggests the disappearance of magnetite phase in the catalyst with reaction time;
- (4) the XRD intensity of the peaks at  $2\theta = 38, 43, 45.0$  and  $73.0^\circ$  grow with increasing reaction time.

The increase in the intensity of the  $38.0$  and  $45.0$  peaks indicate that the  $\text{Fe}_3\text{C}$  and  $\text{Fe}$  phases increase with reaction time. The increase in the peak intensity at  $43^\circ$  indicates the possible formation of another phase. As mentioned above, magnetite decreased with run time. Therefore, if the XRD peak at  $62.5^\circ$  is solely due to magnetite, it should decrease with run time. Instead, the  $62.5^\circ$  peak increases with run time; this indicates the presence of an iron phase having an XRD peak near  $62.5^\circ$ . This, and the observation of an increase in intensity of the  $73^\circ$  peak with run time, strongly suggests the formation of a new phase,  $\text{FeO}$  wustite, which increases with run time.

Figure 2 shows the XRD pattern of the CO activated catalyst following 10 and 48 hrs. in syngas. After 10 hrs of syngas conversion, the XRD pattern (Fig. 2a) shows that magnetite  $\text{Fe}_3\text{O}_4$  is the major phase; weak lines at  $2\theta=38.0$  and  $45.0$  still can be seen. However, the intensity was weaker than that before the introduction of syngas (Fig. 1c). This indicates that a portion of  $\text{Fe}_3\text{C}$  and/or  $\alpha\text{-Fe}$ , produced by reaction of  $\text{Fe}_2\text{O}_3$  with CO, has been oxidized to  $\text{Fe}_3\text{O}_4$  magnetite. Moreover, by comparing Fig. 1c with Fig. 2a, the XRD characteristic of  $\text{FeO}$  has disappeared completely after 10 hrs. in syngas.

Apparently, the presence of syngas caused transformation of FeO to Fe<sub>3</sub>O<sub>4</sub> magnetite. Prolonged reaction in the syngas environment also caused the XRD peaks characteristic of Fe<sub>3</sub>C and  $\alpha$ -Fe to disappear completely (Fig. 2b). Based on the Fe<sub>3</sub>O<sub>4</sub> (311) peak ( $2\theta=35.3^\circ$ ), using the Scherrer equation ( $d=\lambda /w_{1,2}\cos\theta$ ) a mean particle size of 230 Å was estimated for the catalyst after 10 hr syngas reaction. A particle of this size corresponds to a surface area of about 50 m<sup>2</sup>/g (calculated by  $A=6V/d$ ).

Figure 3 shows a typical TEM picture for the catalyst activated in CO followed by 10 hr of syngas reaction. The particle size distribution based on TEM pictures of the sample is presented in Figure 4. A normal distribution of particle sizes can be seen. An average particle size of about 290 Å (calculated by  $(\sum d^3/n)^{1/3}$ ) was obtained. Thus the mean particle size of the catalyst obtained from TEM study shows good agreement with the one estimated from XRD line broadening (230 Å).

Figure 5 shows the evolution of CO<sub>2</sub> as a function of the duration of pretreatment of the Fe<sub>2</sub>O<sub>3</sub> catalyst in CO. The fraction of CO<sub>2</sub> in the exited gas decreases from 2.5 % after 2 hr to 0.5% after 24 hr in CO. This indicates that the reaction of CO with Fe<sub>2</sub>O<sub>3</sub> readily occurs at 260 °C; this observation agrees with the XRD results which show the presence of Fe<sub>3</sub>O<sub>4</sub>, Fe<sub>3</sub>C and Fe in the sample activated in CO for 2hrs (Fig. 1a). The detection of CO<sub>2</sub> in the exited gas after 24 hrs of CO exposure suggests that the conversion of iron oxides to iron carbides is incomplete; this is consistent with the detection of Fe<sub>3</sub>O<sub>4</sub> and FeO by XRD in the sample after 24 hrs of activation in CO (Fig. 1c).

Some of the results of syngas conversion for the catalyst activated in CO are presented in Table 3. Plots of % hydrogen (filled circles) and CO conversions (filled circles) as a function of reaction time are shown in Figure 6a and 6b, respectively. Clearly, the H<sub>2</sub> conversion decreases whereas the CO conversion increases with reaction time. Both CO and H<sub>2</sub> conversion, however, level off at 40% and 22%, respectively, after 10 hr of reaction time. Consequently, the H<sub>2</sub>/CO usage ratio, indicated in table 1 column 4, decreases with time to attain a constant value after 10 hrs of synthesis.

TABLE 3. RESULTS OF SYNGAS REACTION FOR HIGH SURFACE AREA Fe<sub>2</sub>O<sub>3</sub> PRETREATED IN CO<sup>a</sup>

Time (hr)	% Conversion		H <sub>2</sub> /CO Usage	CH <sub>4</sub>	% Selectivity <sup>b</sup>			Olef/Para.	
	CO	H <sub>2</sub>			C <sub>2</sub>	C <sub>3</sub>	CO <sub>2</sub>	C <sub>2</sub>	C <sub>3</sub>
2	12.6	36.3	3.0	21.3	4.3	4.7	40.1	0.32	1.93
10	37.2	24.2	0.68	6.0	2.0	2.7	17.9	0.29	1.15
24	43.1	21.8	0.53	6.3	2.3	3.0	20.4	0.27	0.91
48	39.0	21.8	0.58	6.4	2.0	2.5	17.5	0.26	0.92

a. Reaction conditions: 260°C, 8 atm., CO/H<sub>2</sub> = 1.03, 2.9 l/g-Fe<sub>2</sub>O<sub>3</sub>/hr.

b. Selectivities are based on total CO conversion.

Figure 7a and 7b show CO<sub>2</sub> (filled circles) and CH<sub>4</sub> (filled circles) selectivities, as a function of run time. Both selectivities decrease with run time and level off after 10 hr. From column 9 of Table 1, the C2 olefin/paraffin (o/p) ratio does not change significantly (ca. 10%) with reaction time. The C3 o/p ratio (column 10) decreases with run time and remains constant after 10 h on stream. Comparing column 9 and 10 with column 4 of Table 1, it appears that C2 o/p ratio is not affected significantly by a change in the H<sub>2</sub>/CO usage ratio; however, the other four selectivities and the C3 o/p ratio follow the same trend as that of H<sub>2</sub>/CO usage.

Because of space limitations the activation and conversion of syngas of the sample reduced in hydrogen prior to syngas conversion or the activation in syngas will be described; only a summary of the results will be given below.

### EFFECT OF ACTIVATION GAS ON CATALYST STRUCTURE

The present study shows that Fe<sub>2</sub>O<sub>3</sub> can be partially reduced in CO, in hydrogen or in CO/H<sub>2</sub> mixture. After 10 hr of activation, Fe<sub>2</sub>O<sub>3</sub> was completely transformed to Fe<sub>3</sub>O<sub>4</sub> and other phases. The ease of reduction of Fe<sub>2</sub>O<sub>3</sub> to Fe<sub>3</sub>O<sub>4</sub> has been well documented (14,15), and is expected on the basis of the exothermic nature of the reaction (14).

XRD studies conducted in the present work clearly indicate that CO is a better reducing agent, as well as a carburization agent, than H<sub>2</sub> or the H<sub>2</sub>/CO mixture. These results are consistent with a static TG/DTA study which showed that CO is better than H<sub>2</sub> for the reduction of  $\alpha$ -Fe<sub>2</sub>O<sub>3</sub> (14). The incomplete transformation of Fe<sub>2</sub>O<sub>3</sub> to iron carbide after 24 hrs. of activation in CO (Fig. 1c) is also consistent with a Mössbauer spectroscopic study that showed the presence of magnetite Fe<sub>3</sub>O<sub>4</sub> and Fe<sub>5</sub>C<sub>2</sub> in an amorphous  $\alpha$ -Fe<sub>2</sub>O<sub>3</sub> after 24 hrs of activation in CO at 270 °C (15). However, Zarochak and McDonald have reported a complete transformation of Fe in a Fe-K-Cu (65:0.29:0.6) catalyst to carbidic iron at 280 °C and under 200 psig CO during 24 h in a slurry phase autoclave (13). The presence of K, which has been reported to accelerate carburization (16,17), as well as the higher temperature (280 vs 260 °C) and pressure (200 vs 105 psig) they used, may explain the difference between their and our results.

The observation of only a small fraction of metallic iron after 24 h activation in H<sub>2</sub> at 260 °C is surprising, but this has also been reported (15). It is possible that the condenser in the reactor set-up which was used to trap tetralin vapor may also condense water vapor during the course of reaction; this water may reoxidize metallic Fe to Fe<sub>3</sub>O<sub>4</sub>.

### EFFECT OF SYNGAS REACTION ON THE CATALYST STRUCTURE

After 10 h of syngas conversion, the catalysts activated in hydrogen and CO showed only the Fe<sub>3</sub>O<sub>4</sub> phase by XRD. The catalyst without preactivation also showed by XRD only the Fe<sub>3</sub>O<sub>4</sub> after 48 hr on stream. The observation of only Fe<sub>3</sub>O<sub>4</sub> phase for iron catalysts after syngas conversion has been reported for catalysts which showed mainly iron carbide or  $\alpha$ -Fe phase after activation (13,18). This has been attributed to the presence of water vapor, particularly at high conversion. As mentioned in the previous section, the condenser set-up can accumulate relatively large amount of water. High water vapor

pressure in the reactor is thus expected. This may be one of the reason for the detection only  $\text{Fe}_3\text{O}_4$  phase by XRD in the catalysts after prolonged syngas conversion.

Earlier study of Fe catalysts often observed carbidic phase in the spent catalysts (19,20). However, the catalysts in those studies are low surface area material or contain alkali promoters. An outer layer of large particles of catalysts may retard oxidation of carbidic or metallic phase. The alkali promoter which has been reported to accelerate carburization is also expected to stabilize the carbidic phases. Thus in the present study, the use of higher surface area  $\text{Fe}_2\text{O}_3$  and the lack of alkali promoter in the catalyst, may also be the reasons for the observation of only  $\text{Fe}_3\text{O}_4$  by XRD in the catalysts after 10 or more hours of syngas conversion.

The average particle size of  $\text{Fe}_3\text{O}_4$  was 230, 250 and 310Å for catalyst activated in CO and in  $\text{H}_2$  followed by 10 h syngas conversion, and direct activation in syngas for 48 h, respectively. Therefore, the activation does not significantly impact on the particle size of the catalysts following syngas conversion.

#### EFFECT OF PRETREATMENT ON CO HYDROGENATION SELECTIVITY AND ACTIVITY

It appears that in the earlier stage of syngas conversion, the  $\text{CO}_2$  and methane selectivities for the catalysts activated in CO or without preactivation were similar and higher than that of the  $\text{H}_2$ -activated catalyst. However, the two selectivities merge after only 10 h of syngas conversion so that the catalysts prepared by the three activation procedures become the same. Thus the gas(es) used for activation appear to affect the product selectivity primarily in the earlier stage of syngas reaction. The time dependant trend and magnitude of  $\text{CH}_4$  and  $\text{CO}_2$  for the catalyst activated in CO and without preactivation indicates that they have similar active phases. Furthermore, independent of pretreatment, both  $\text{CH}_4$  and  $\text{CO}_2$  selectivities merged after 10 h in syngas. This implies that the active sites in the catalysts are similar after 10 h of syngas conversion.

The catalysts activated in hydrogen and without preactivation have comparable CO and hydrogen conversion after 24 h on stream. The catalyst activated in CO or without preactivation showed an induction period; however, no induction period was observed for the hydrogen pretreated catalyst. The CO conversion was similar for the catalyst activated in  $\text{H}_2$  or that was not pretreated; however, the CO pretreated catalyst has a CO conversion ca. 3 times that of the sample activated in syngas or hydrogen. Thus, the present study clearly shows that, for a high surface area  $\text{Fe}_2\text{O}_3$  in a CSTR using tetralin as solvent, activation in CO produced the most active catalyst for subsequent CO hydrogenation. The results are consistent with the studies of the effect of activation procedure on FT activity for promoted K-Cu- $\text{Fe}_2\text{O}_3$  catalysts (12,13) and for a FeMn catalyst (21). The catalyst activated in  $\text{H}_2$  has a CO conversion comparable to that of a catalyst without preactivation and is in agreement with the results obtained by Dictor and Bell (19).

The XRD patterns show that only  $\text{Fe}_3\text{O}_4$  is detected for the catalyst at the point of maximum activity, and this does not depend upon the activation gases. This implies that  $\text{Fe}_3\text{O}_4$  is the active phase, or that the active phase can not be detected by XRD. However, the fact that, after 2 h in syngas,  $\text{Fe}_2\text{O}_3$  already has been completely transformed into

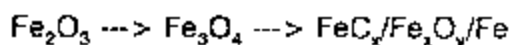
$\text{Fe}_3\text{O}_4$  and that this material only shows minimum activity while a  $\text{Fe}_3\text{O}_4$  phase that was observed for the catalyst activated in  $\text{H}_2$  for 24 h showed a much higher activity, indicates that bulk  $\text{Fe}_3\text{O}_4$  is not likely to be the active phase for CO hydrogenation. Furthermore, at maximum activity, the particle size of  $\text{Fe}_3\text{O}_4$  for the catalyst activated in CO was 74% of that for the catalyst activated in hydrogen. The CO conversion for the CO activated catalyst however, was 3 times that of the catalyst activated in hydrogen. Therefore, the presence of an active surface or bulk phase supported on the surface of  $\text{Fe}_3\text{O}_4$  is likely.

The attainment of a similar selectivity independent of the initial pretreatment in the present study suggests the same, or at least similar active phase(s). It has been proposed that under reaction conditions, a number of compounds coexists on the surface of an iron catalyst: iron oxides, iron carbides and metallic iron co-exist (22). Iron carbides has been proposed to be the active phase (23-25) and the fraction of iron carbides on the catalyst surface determines the activity (24). Others, however, have proposed that metallic iron (26,27), or iron oxides (28-30) are the active phases. In the present study, the nature of the active sites was not determined. Nevertheless, the present study suggests that a common active phase can be obtained after a period of syngas conversion.

We speculate that the  $\text{Fe}_2\text{O}_3$  catalyst pretreated in  $\text{H}_2$  resulted in the following transformation:



Pretreatment of the  $\text{Fe}_2\text{O}_3$  catalyst in CO or syngas results in the following transformations:



The difference among the activities of catalysts appears to depend upon the concentration of active sites on the surface. Apparently,  $\text{Fe}_2\text{O}_3$  activated in CO produced the highest concentration of active sites, and therefore results in the highest activity.

## CONCLUSIONS FOR PRETREATMENT

The present study has shown that activation of a high surface area  $\text{Fe}_2\text{O}_3$  catalyst in CO in a CSTR using tetralin as solvent results in an activity that is three times of material that is activated in  $\text{H}_2$  or directly in the syngas.

Independent of the catalyst activation, similar methane and  $\text{CO}_2$  selectivities are obtained. This suggests that the active catalytic phase is the same. Since particle size estimated by XRD only shows a variation within 30%, the difference among the activities of the differently activated catalysts can be attributed to differences in the concentration of active sites on the catalyst surface.

## PRECIPITATION OF IRON CATALYST

Preliminary to doing continuous precipitation in which seeding occurs, we prepared a batch sample that will serve as the seed. This was done to learn the properties so the

potential seed material. To accomplish this, 1460g of  $\text{Fe}(\text{NO}_3)_3 \cdot 9\text{H}_2\text{O}$  in 6L distilled deionized (DD) water (approx. 0.6M) was added to a 5 gal. bucket containing 900 mL of ammonium hydroxide (29%) while stirring. The final pH of the solution was 7.13 and care was taken to keep the pH above 7. Total time for base addition was approximately 10 min.

Filtration of the solution required several hours. Five samples (approx. 84g each) were taken of the moist filter cake for ion exchange and the remainder was added to DD water and stirred. This fraction was filtered. 5 more samples taken, remainder washed, etc. until the final product had been washed and filtered 3 times.

Ion exchange was accomplished by adding a pre-weighed amount of precipitate (84 grams, approximate) to stirring beakers containing 250 mL of aqueous  $\text{KNO}_3$  at different concentrations (1, 3, 5, 8, or 10 wt.%). After stirring approximately 5 min. the solutions were filtered (gravity) and the aqueous fraction analyzed for Fe and K. The amount of K adsorbed on the solid was calculated from the difference in the K level in the starting solution and the solution separated from the solid that was separated from the solid. Solid fractions were collected and air dried.

The final product was dried and heated several ways:

- 1) Dried in a vacuum oven at room temperature for at least 2 hours and then gradually increased the temperature to approx. 100°C.
- 2) Vacuum dried as above then admitted to a tube, flushed with He for 1 hr., heated rapidly to 285°C, held for at least 4 hrs. then cooled under He.
- 3) Vacuum dried as in (1), heated as in (2) only to 295°C.
- 4) Dried overnight in a drying oven at atmospheric pressure at approximately 110°C.

Fig. 8 shows the effects of these treatments on surface area and pore volume. A significant surface area is obtained by removing water slowly under vacuum. About 40% of the surface area is lost on subsequent heating to 285°C and an additional 33% is lost by increasing the temperature another 10°. This trend is also seen by TGA/MS (Fig. 9). The sample used in this experiment was one prepared in a small scale batch (sample #IC2) and dried in a drying oven. The major weight losses occur at 100°C and again after 10 min. at 300°C under He flow corresponding to the evolution of water and  $\text{CO}_2$  as well a compound with a mass of 16. Interestingly, the total pore volume as measured by  $\text{N}_2$  adsorption shows the opposite trend as the BET surface area. This must be the result of formation of larger particles and their contact zones. Particle size as measured from XRD line broadening (Scherrer eqn.) and major pore radius as calculated from  $\text{N}_2$  desorption (using bcc crystal structure reported for alpha- $\text{Fe}_2\text{O}_3$ ) are shown in Fig. 10. Increasing the severity of heating results in larger crystals and larger pores, with the oven dried sample falling between the vacuum dried samples heated to 285°C and 295°C.

Iron oxides tested for ion exchange capacity were split into five equal fractions weighing approximately 84 g each. These were added to vessels containing 250 mL of aqueous  $\text{KNO}_3$  in varying concentrations (1%, 3%, 5%, 8%, or 10% by weight). The solutions were stirred for 5 minutes prior to filtration. The filtrate was collected and analyzed for K and Fe content by Inductively Coupled Plasma Spectroscopy (ICP). Adsorbed potassium is defined as the difference in K between the final filtrate solution and the starting  $\text{KNO}_3$  solution per gram of wet iron oxide precipitate. For a 10%  $\text{KNO}_3$  solution, about 2 wt.%  $\text{K}^+$  ( $\sim 2.5$  wt.%  $\text{K}_2\text{O}$ ) was present on the solid.

## REFERENCES

1. H. H. Storch, N. Columbic and Robert B. Anderson, "The Fischer-Tropsch and Related Syntheses," John Wiley & Sons, Inc., New York, NY, 1951, p. 115).
2. H. Pichler and A. Hector, Kirk-Othmer Encyclopedia of Chemical Technology, Wiley & Son, New York, NY, Vol. 14, pp. 446-489).
3. F. Haber and R. LeRossignol, Ber., 40, 2144 (1907).
4. A. Mittasch, Advan. Catal., 2, 82, (1950).
5. Clarke, Sister Margaret Jackson, "The Federal Government and the Fixed Nitrogen Industry 1919-1926", Ph.D. Thesis, Oregon State University, Corvallis, OR, June, 1977.
6. P. H. Emmett in "Heterogeneous Catalysis. Selected American Histories, (B. H. Davis and W. P. Hettinger, Jr., Eds.), ACS Symp. Series, 222, 195 (1982).
7. A. T. Larson, Chem. Met. Eng., 30, 948 (1924).
8. R. B. Anderson in "Catalysis," (P. H. Emmett, Ed.) Reinhold Pub. Corp., New York, NY, Vol. 4, 1956, p 148.
9. R. B. Anderson in "Catalysis", (P. H. Emmett, Ed.), Reinhold Pub. Corp., New York, NY, 1956, pp. 119-120.
10. M. E. Dry in "Catalysis. Science and Technology", (J. R. Anderson and M. Boudart, Eds.) Springer-Verlag, Berlin, Vol. 1, (1981), p. 159.
11. R. B. Anderson in "Catalysis" (P. H. Emmett, Ed.) Van Nostrand Pub. Co., 1956, Vol. 4, pp 29-255.
12. D. B. Bukur, X. Lang, J. A. Rossin, W. H. Zimmerman, M. P. Rosynek, E. B. Yeh and C. Li, Ind. Eng. Chem. Res. 28 1130-1140 (1989).
13. M. F. Zarochak and M. A. McDonald, Proceed. Indirect Liquefaction Contractor Meeting, Dec 1986, Pittsburgh, pp 58-82.

14. M. A. Richard, S. L. Soled, R. A. Fiato and B. A. Derites, *Mat. Res. Bull.*, Vol 18, pp 829-833 (1983).
15. F. J. Berry and M. R. Smith, *J. Chem. Soc. Faraday Trans. 1*, 85(2) 467-477 (1989).
16. H. Pichler and H. Merkel, US Bureau of Mines Tech. Paper 718 (1949).
17. G. L. Vogler, X.-Z. Jiang, J. A. Dumesic and R. J. Madon, *J. Catal.* 89 116 (1984).
18. M. H. Jellinek and I. Frankuchen in "Advance in Catalysis", Vol 1, Academic Press, 279 (1948).
19. R. A. Dictor and A. T. Bell, *J. Catal.* 97 121-136 (1986).
20. R. B. Anderson in "Catalysis" edited by P. H. Emmett, Van Nostrand-Reinhold, New York, 1956, Vol IV, pp 29-255.
21. H. W. Pennline, M. F. Zarochak, J. M. Stencel and J. R. Diehl, *Ind. Eng. Chem. Res.* 26 595-601 (1987).
22. J. W. Niemantsverdriet, C. F. J. Flipse, A. M. Van Der Kraan and J. J. Van Loef, *Appl. Surf. Sci.* 10 302-313 (1982).
23. G. B. Raupp and W. N. Delgass, *J. Catal.* 58 348 (1979).
24. J. W. Niemantsverdriet and A. M. Van Der Kraan, *J. Catal.* 72 385-388 (1981).
25. D. J. Dwyer and J. H. Hardenbergh *J. Catal.* 87, 66-76 (1984).
26. D. J. Dwyer and G. A. Somorjai *J. Catal.* 52 291 (1978).
27. H. J. Kerbs, H. P. Bonzel and G. Gafner, *Surface. Sci.* 88 269 (1979).
28. J. P. Reymond, P. Meriadeau and S. J. Teichner, *J. Catal.* 75 39-48 (1982).
29. F. B. Blanchard, J. P. Raymond, B. Pommier, and S. J. Teichner, *J. Mol. Catal.* 17 171-181 (1982).
30. L. J. E. Hofer; in "Catalysis" edited by P. H. Emmett, Van Nostrand-Reinhold, New York, 1956, Vol IV, pp 373-441.



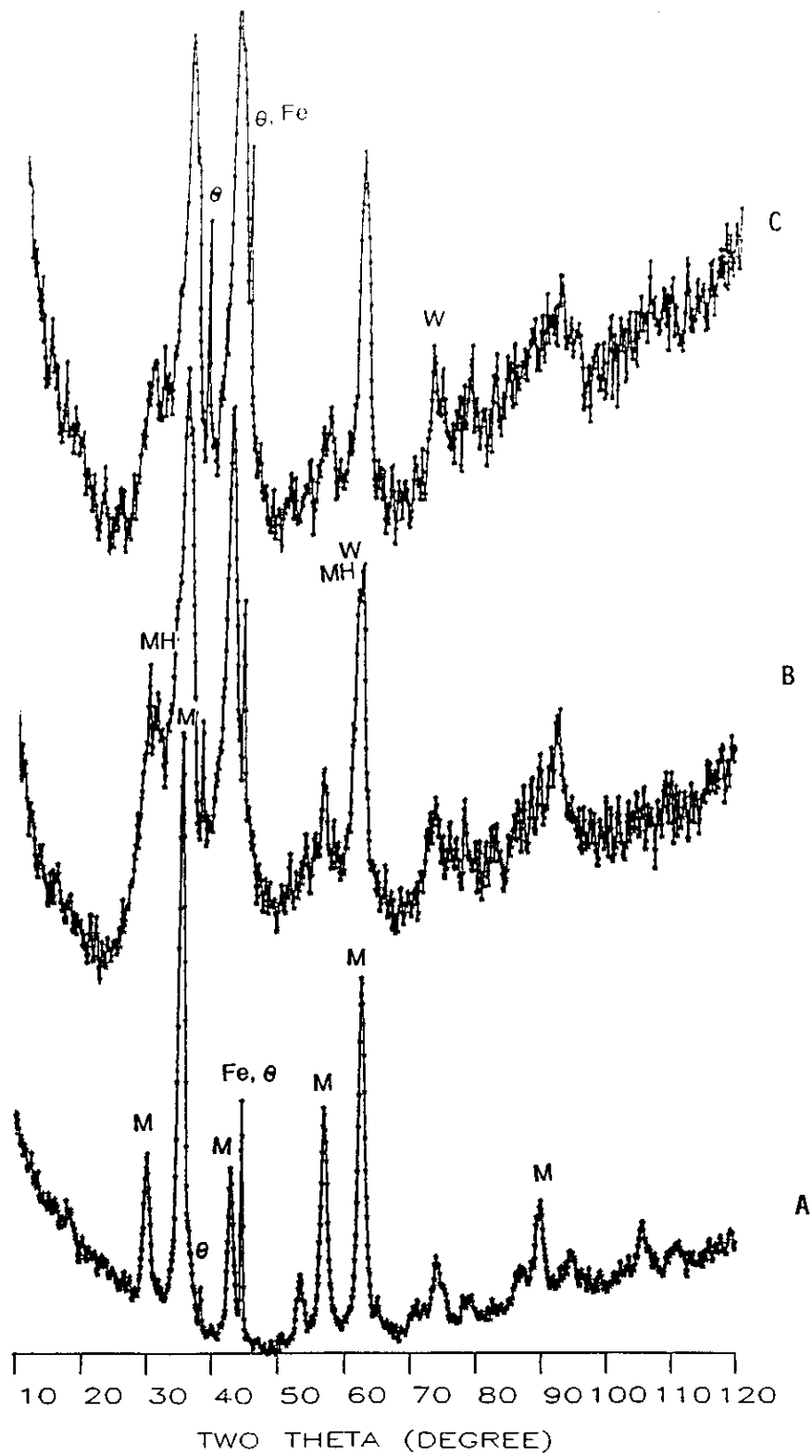


Figure 1. XRD patterns of the material withdrawn after 2 (A), 10 (B) and 24 hr. (C) in CO at 8 atm and 260°C.

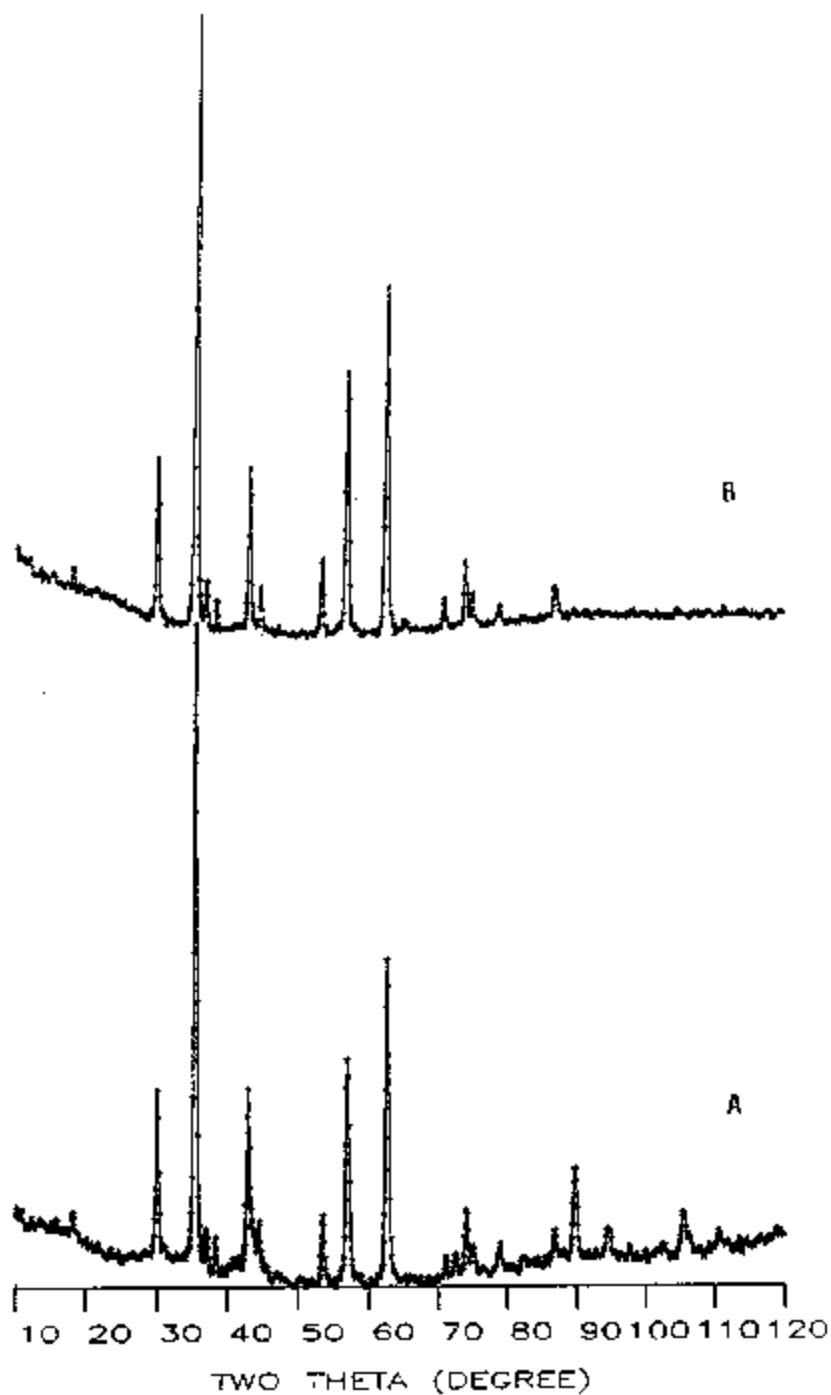


Figure 2. XRD patterns of the 24 hr. CO pretreated sample (figure 1C) following 10 (A) and 48 hrs. (B) in syngas ( $H_2/CO = 1.03$ ) and 8 atm and 260°C.



450A

Figure 3. Typical TEM picture of a material pretreated in CO and expressed to syngas for 10 hrs.

Figure 4. Size distribution of particles in figure 3.

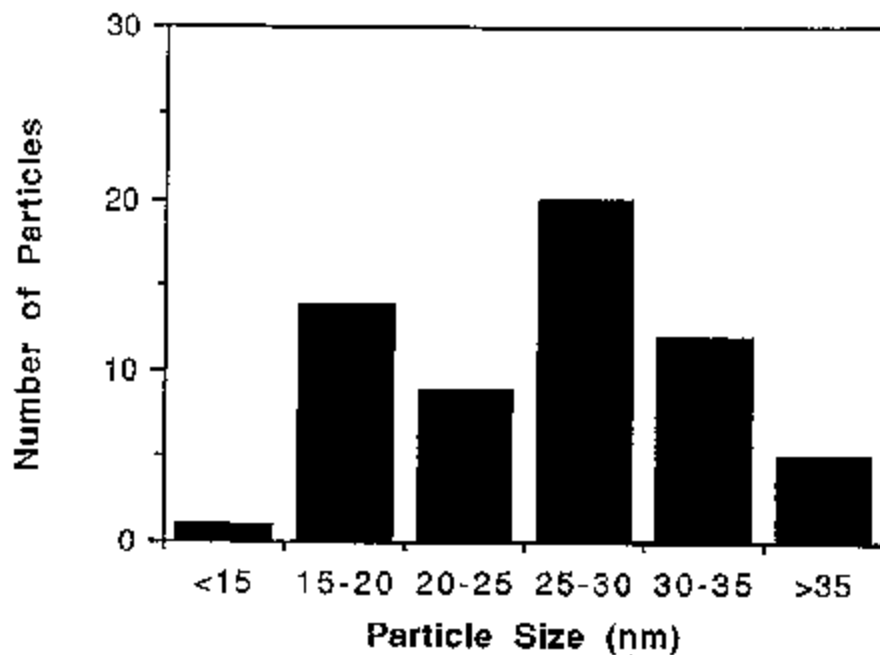
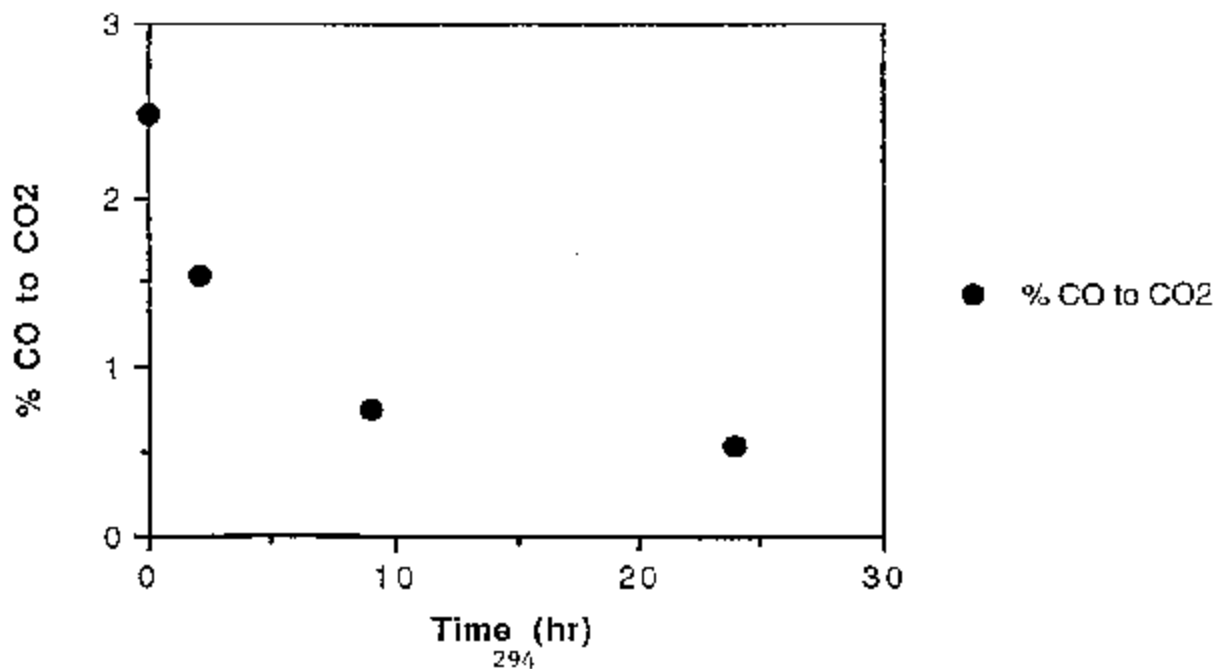


Figure 5. CO<sub>2</sub> in exit gas during activation in CO at 260°C and 8 atm.



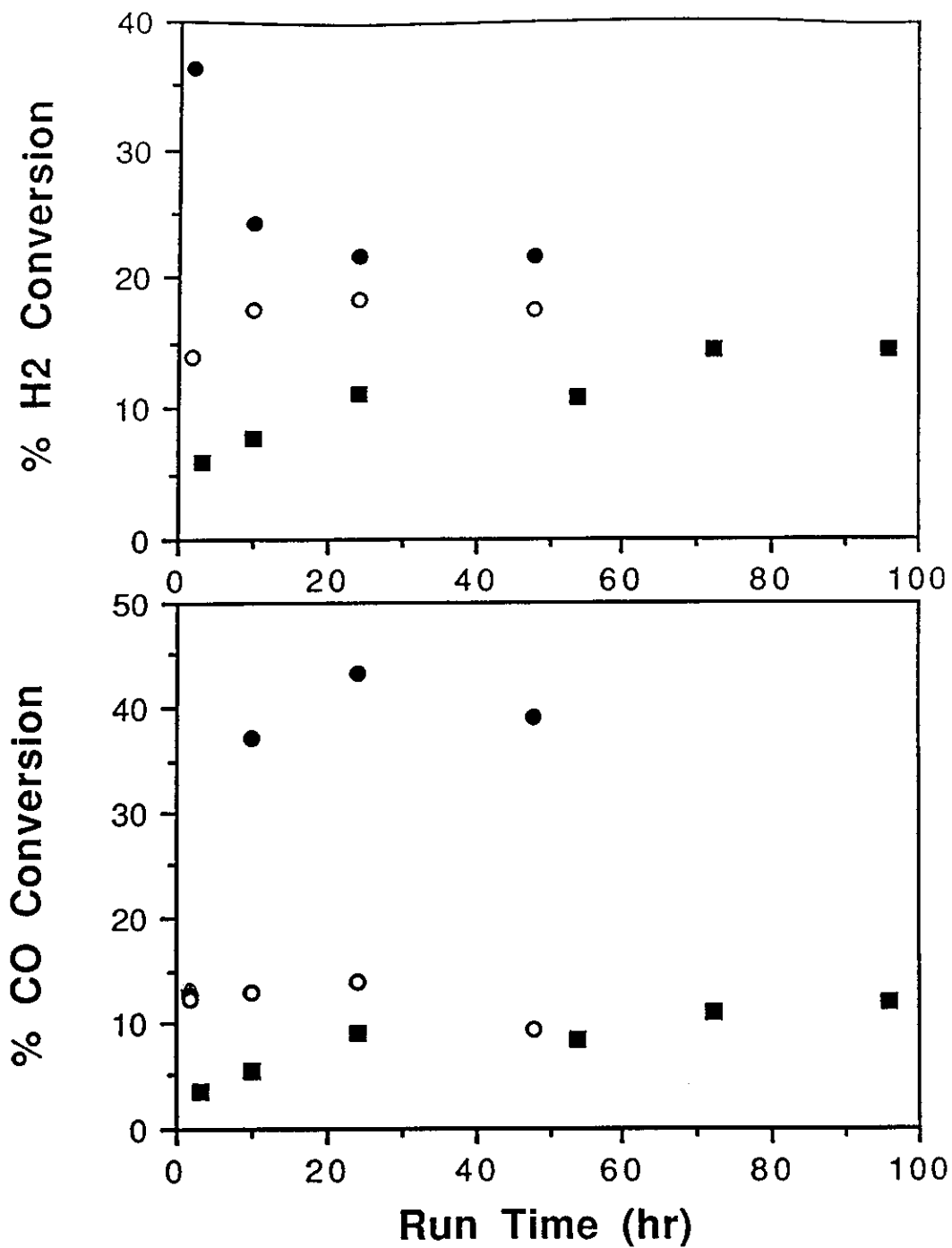


Figure 6. A (top). Hydrogen conversion (%) of the catalyst activated in CO (●), H<sub>2</sub> (○) or CO/H<sub>2</sub> (■). B (bottom). CO conversion (%) of the catalyst activated in CO (●), H<sub>2</sub> (○) or CO/H<sub>2</sub> (■).

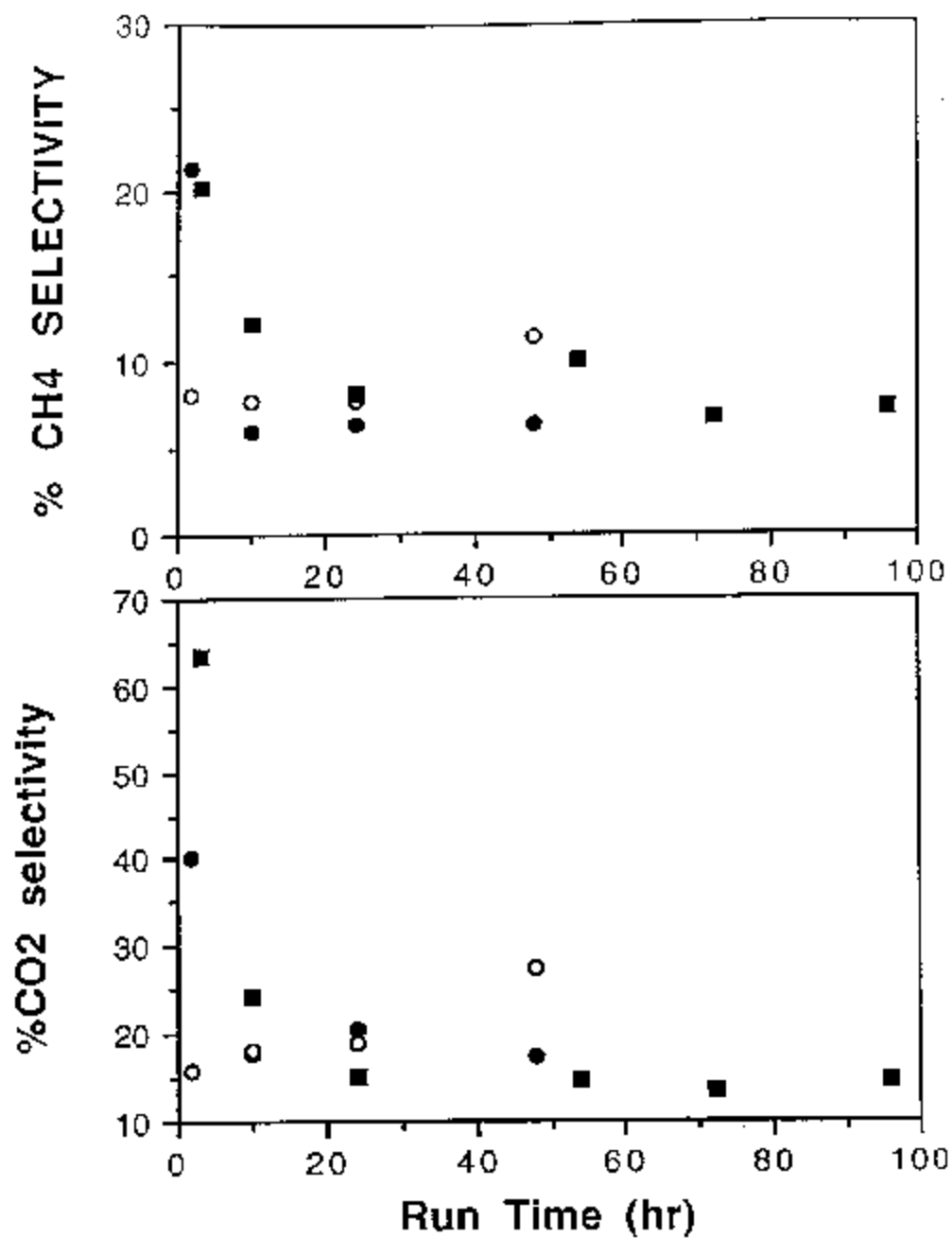
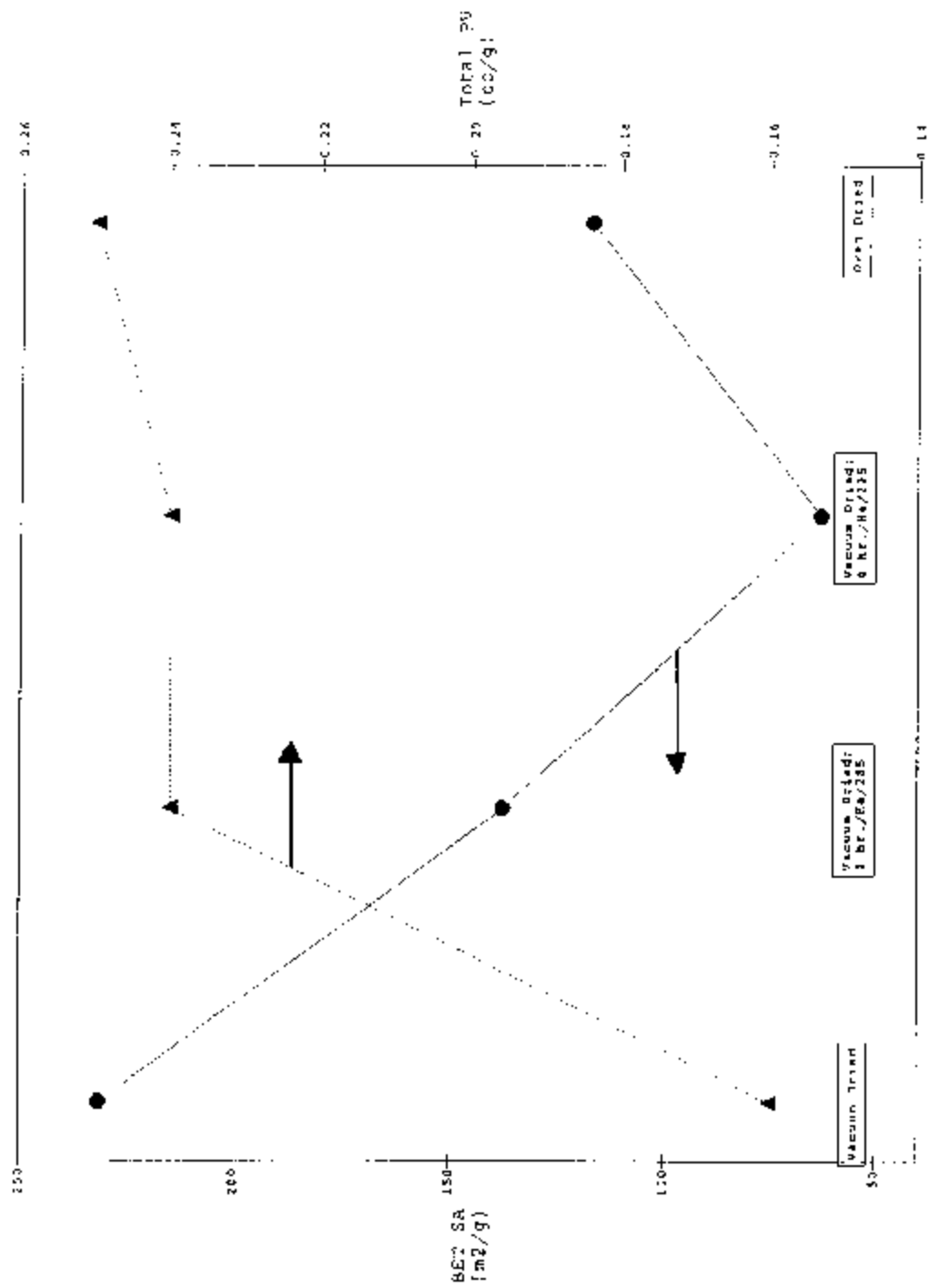


Figure 7. A (top). CO<sub>2</sub> formation for catalyst activated in CO (●), H<sub>2</sub> (○) or CO/H<sub>2</sub> (■). B (bottom). CH<sub>4</sub> formation for catalyst activated in CO (●), H<sub>2</sub> (○) or CO/H<sub>2</sub> (■).

Figure 8. Effects of drying on the BET surface area and the total pore volume of a precipitated iron oxide.



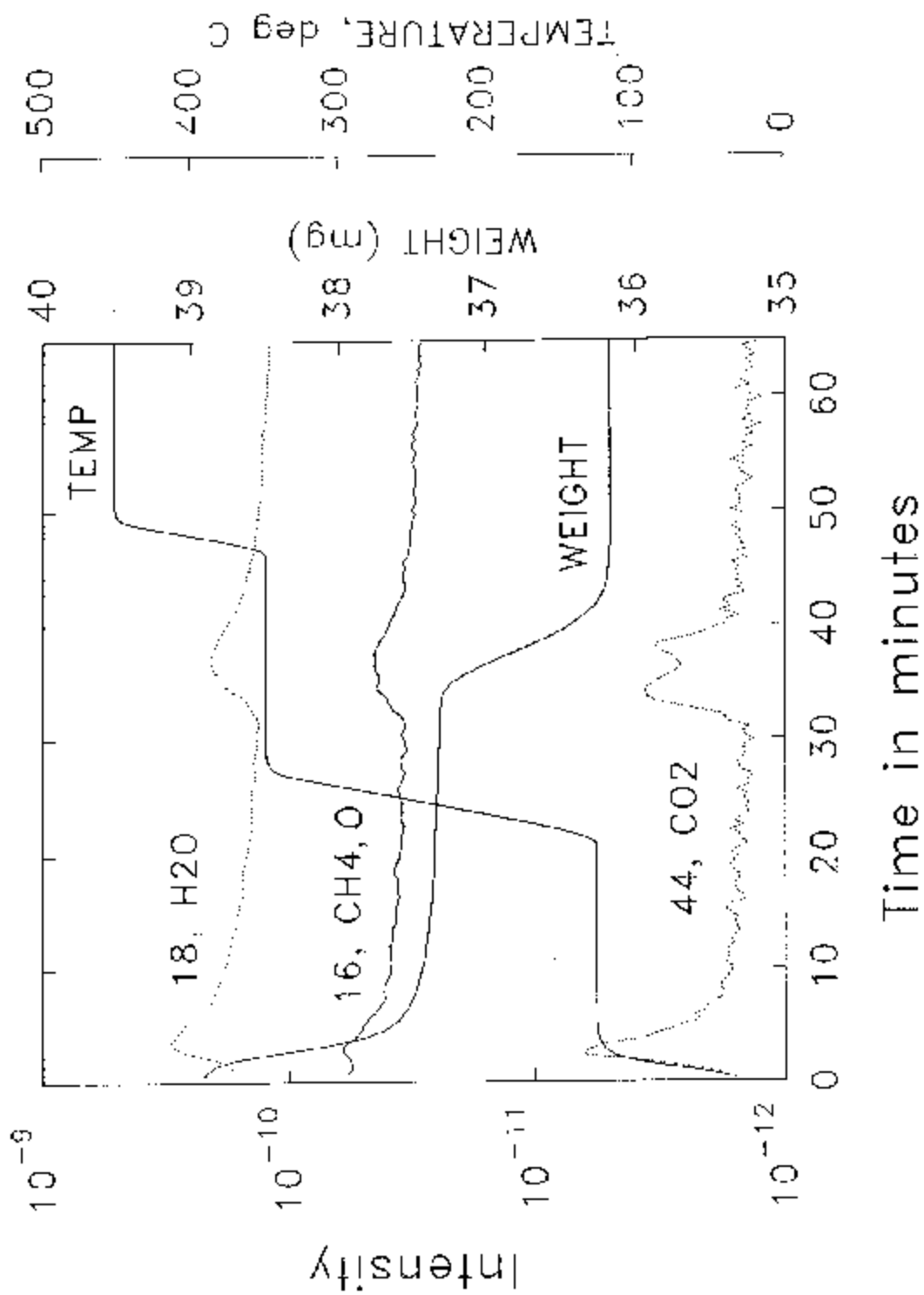


Figure 9. TGA/MS analysis of a precipitated iron oxide dried at 110°C at ambient pressure.



Figure 10. Effects of drying on particle size (determined from XRD) and major pore size (determined by nitrogen desorption) on a precipitated iron oxide.

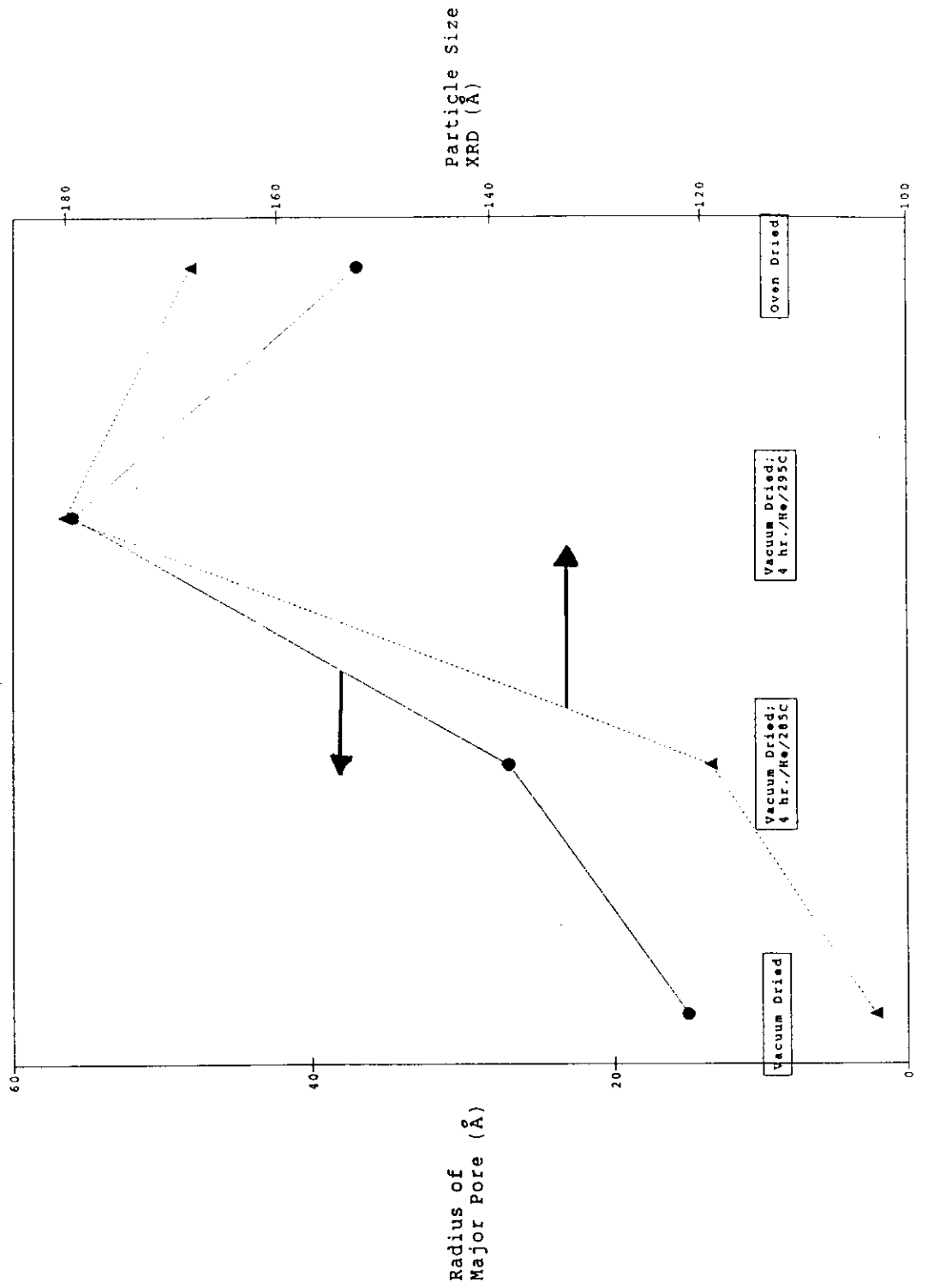


Figure 3. Typical TEM picture of a material pretreated in CO and expressed to syngas for 10 hrs.

